The subcellular localization of acetyl-CoA carboxylase 2

Lutfi Abu-Elheiga*, William R. Brinkley†, Ling Zhong†, Subrahmanyam S. Chirala*, Gebretateos Woldegiorgis‡, and Salih J. Wakil*§

*Verna and Marrs McLean Department of Biochemistry and Molecular Biology and †Department of Molecular and Cellular Biology, Baylor College of Medicine, One Baylor Plaza, Houston, TX 77030; and ‡Department of Biochemistry and Molecular Biology, Oregon Graduate School of Science, Box 91000, Portland, OR 97291

Contributed by Salih J. Wakil, December 9, 1999

Animals, including humans, express two isoforms of acetyl-CoA carboxylase (EC 6.4.1.2), ACC1 (M_r = 265 kDa) and ACC2 (M_r = 280 kDa). The predicted amino acid sequence of ACC2 contains an additional 136 aa relative to ACC1, 114 of which constitute the unique N-terminal sequence of ACC2. The hydropathic profiles of the two ACC isoforms generally are comparable, except for the unique N-terminal sequence in ACC2. The sequence of amino acid residues 1–20 of ACC2 is highly hydrophobic, suggesting that it is a leader sequence that targets ACC2 for insertion into membranes. The subcellular localization of ACC2 in mammalian cells was determined by performing immunofluorescence microscopic analysis using affinity-purified anti-ACC2-specific antibodies and transient expression of the green fluorescent protein fused to the C terminus of the N-terminal sequences of ACC1 and ACC2. These analyses demonstrated that ACC1 is a cytosolic protein and that ACC2 was associated with the mitochondria, a finding that was confirmed further by the immunocolocalization of a known human mitochondria-specific protein and the carnitine palmitoyltransferase 1. Based on analyses of the fusion proteins of ACC–green fluorescent protein, we concluded that the N-terminal sequences of ACC2 are responsible for mitochondrial targeting of ACC2. The association of ACC2 with the mitochondria is consistent with the hypothesis that ACC2 is involved in the regulation of mitochondrial fatty acid oxidation through the inhibition of carnitine palmitoyltransferase 1 by its product malonyl-CoA.

Acetyl-CoA carboxylase (ACC) catalyzes the carboxylation of acetyl-CoA to form malonyl-CoA, an intermediate substrate that plays a pivotal role in the regulation of fatty acid metabolism. Besides its role in the biosynthesis of long-chain fatty acids (1–3), malonyl-CoA has been implicated in the regulation of the carnitine palmitoyl-CoA shuttle system that is involved in the mitochondrial β-oxidation of long-chain fatty acids. In animals, two isoforms of the carboxylase have been identified, ACC1 (M_r = 265,000) and ACC2 (M_r = 280,000) (4, 5). The two enzymes are encoded by separate genes and display distinct tissue distribution and regulation (6–9). The ACC1 carboxylases are highly expressed in lipogenic tissues, such as liver and adipose, and their levels are regulated transcriptionally while their activities are regulated posttranslationally by phosphorylation/dephosphorylation of selected serine residues and by allosteric regulation through the action of citrate and palmitoyl-CoA (10–18). Dietary and hormonal states of the animal affect the level and activities of the ACC1 enzymes. A carbohydrate-rich, low-fat diet stimulates the expression and activities of ACC1, whereas starvation and diabetes reduce the ACC1 activities by repressing the expression of the ACC1 gene or by increasing the phosphorylation levels of the ACC1 protein (or both). Treating diabetic animals with insulin increases the activity of the enzyme either by dephosphorylation of the protein or by activation of it with citrate (or both), and prolonged insulin treatment stimulates the synthesis of ACC1 protein.

The ACC2 carboxylase was discovered by Thampy (4) in rat heart, an organ in which little or no *de novo* fatty acid synthesis takes place (19, 20). Like ACC1, the ACC2 carboxylase activity is regulated by phosphorylation/dephosphorylation and by citrate (4, 21). Anti-ACC1 antibodies do not bind to ACC2 in a Western blot, nor do they inhibit ACC2 activity (4), suggesting that they are immunologically different (4, 7, 21, 22), even though their amino acid sequences are about 70% similar (7). The ACC2 carboxylase is expressed in liver but is the predominant form of carboxylase in heart and skeletal muscle (5, 7, 9). This finding concurs with the suggestion that the carboxylase is not only a key enzyme in fatty acid synthesis (1) but also plays an important role in regulating fatty acid oxidation (23, 24). In the latter role, malonyl-CoA, the product of ACC, is a potent inhibitor of carnitine palmitoyltransferase 1 (CPT1), an enzyme that is located on the mitochondrial membrane and generates palmitoylcarnitine and free CoASH. Palmitoylcarnitine is transported across the inner mitochondrial membrane in exchange for carnitine by the carnitine carrier and is reconverted into palmitoyl-CoA in a reaction catalyzed by carnitine palmitoyltransferase 2 (CPT2), an enzyme located on the matrix side of the inner mitochondrial membrane. The carnitine palmitoyl-CoA shuttle system is the first step in bringing long-chain fatty acids to the β-oxidation system (24) for energy production. Regulation of this shuttle pathway through malonyl-CoA becomes an important physiological process for interrelating lipid and carbohydrate metabolism in animals.

Recently, the cDNAs encoding human ACC1 and ACC2 were cloned and sequenced (6, 7, 9). When the predicted amino acid sequences of the two isoforms were compared, the most significant difference found between them was the extra 114 aa in the N terminus of ACC2 (7). The finding that the N-terminal amino acid sequence of ACC2 begins with hydrophobic residues suggests that the ACC2 isoform is a membrane-targeted enzyme. This assumption is consistent with the current presumed role of ACC2 in regulating fatty acid oxidation by providing malonyl-CoA, the regulator of CPT1 activity. Because CPT1 is associated with the mitochondrial membrane, it was assumed that ACC2 also might be associated with the mitochondria. The availability of affinity-purified polyclonal antibodies raised against the N-terminal peptide of ACC2 (amino acid residues 1–222) that reacted specifically with ACC2 derived from human, rat, and mouse tissues made it possible for us to test the subcellular location of ACC2 and to compare it with that of ACC1 by using immunofluorescence confocal microscopy. The results presented in this communication show that ACC2, along with CPT1, indeed is associated with the mitochondria.

Abbreviations: ACC, acetyl-CoA carboxylase; CPT, carnitine palmitoyltransferase; GFP, green fluorescent protein; DAPI, 4′,6-diamidino-2-phenylindole; TXRD, Texas Red.

§To whom reprint requests should be addressed at: Department of Biochemistry and Molecular Biology, Baylor College of Medicine, One Baylor Plaza, MS 357A, Houston, TX 77030. E-mail: swakil@bcm.tmc.edu.

The publication costs of this article were defrayed in part by page charge payment. This article must therefore be hereby marked "*advertisement*" in accordance with 18 U.S.C. §1734 solely to indicate this fact.

Materials and Methods

Materials. All restriction enzymes and T_4 DNA ligase were purchased from New England Biolabs. TALON resin and the pEGFP-N1 vector were obtained from CLONTECH. Cell culture medium and sera were purchased from GIBCO/BRL. The human HepG2 and T47D cell lines were obtained from Baylor College of Medicine's tissue culture facility, and the rat neonatal cardiomyocytes were provided by Maha Abdellatif in the Section of Cardiology in the Department of Medicine at Baylor College of Medicine. Propidium iodide and 4′,6-diamidino-2-phenylindole (DAPI) were purchased from Sigma, and the Vectashield antifade mounting medium was from Vector Laboratories. All other chemicals used were of the highest quality commercially available.

Antibodies. A cDNA fragment (nucleotides 1–666) that encodes the N-terminal region of ACC2 was cloned into the pET32-a plasmid and expressed in *Escherichia coli* strain BL21, and the thioredoxin fusion protein was purified and used to raise polyclonal antibodies in rabbits (7). The antiserum was affinity-purified by using the purified fusion protein coupled to cyanogen bromide-activated Sepharose. The purified antibodies recognized ACC2 in a Western blot and in an ELISA. The anti-human heart muscle M-CPT1 polyclonal antibodies were produced as described previously (25). mAbs (MAB1273) raised against the human mitochondrial 66-kDa protein were purchased from Chemicon. The goat anti-rabbit IgG-Texas Red (TXRD) conjugate and the goat anti-mouse IgG-TXRD conjugate were obtained from Molecular Probes. The goat anti-rabbit IgG-FITC conjugate was purchased from Pierce.

Immunofluorescence Microscopy. To avoid artifacts in the microscopic assessment of the intracellular localization of the different proteins, we used the immunocytochemical protocol of Van Hooser and Brinkley (26) that involved fixing the cells in formaldehyde before permeabilizing them with detergent. Human HepG2 cells, human T47D cells, and rat neonatal cardiomyocytes (2×10^5 cells each) were seeded on glass coverslips coated with polyamino acids. The slides were placed in DMEM culture medium containing 10% FBS, and the cells were allowed to grow for 2–3 days until they reached a semiconfluent state. The cultured cells were washed in PBS and then fixed with 4% formaldehyde in PBS for 20 min at room temperature. The fixed cells were treated with 0.5% Triton X-100 in PBS for 30 min at room temperature and incubated for 1 h at 37°C with the primary antibodies, which had been diluted 1:100 in PBS containing 1% BSA. After the primary antibodies were removed, the cells were washed with PBS and incubated for 45 min at 37°C with goat anti-rabbit IgG conjugated to FITC only or together with goat anti-mouse IgG conjugated to TXRD; both secondary antibodies had been diluted 1:20 in PBS containing 1% BSA. The nuclear DNA was counterstained with 5 μg/ml DAPI. Microscopic images were collected by using a Zeiss Axiophot fluorescence microscope equipped with a high-resolution, three-chip Hamamatsu charge-coupled device camera. The images then were digitally processed by using Adobe PHOTOSHOP software and printed on a Codonics NP 1600 dye-diffusion color printer.

Mouse skeletal muscle tissues were sectioned, frozen in liquid nitrogen, and prepared for immunostaining as described above. Once stained, the cells were scanned at 488 nm under a confocal microscope through a series of focal points by using a laser light source.

Cloning of the N-Terminal Region of the Human ACC2 and ACC1 cDNAs into pEGFP. A 1,250-bp cDNA fragment coding for the N-terminal region of human ACC2 was obtained by digesting the ACC2 cDNA with *Xho*I and *Pst*I and subcloning it in-frame with the 5′ end of the green fluorescent protein (GFP) cDNA into pEGFP-N1, which had been linearized with the same restriction enzymes, thereby generating the pEGFP-N1-ACC2-N plasmid. The 5′ end of human ACC1—including the ATG translation initiation codon, a 416-bp *SSt*1-*Sph*I fragment—was cloned in-frame with the *Sph*I-*Pst*I fragment of ACC2 (nucleotides 826–1,250) in pBluescript vector, thus producing a hybrid cDNA clone. The new *Sst*I-*Pst*I fragment was cloned in-frame with the 5′ end of the GFP cDNA, thereby generating the pEGFP-N1-ACC1-N plasmid.

Cell Culture Transfection. Human HepG2 cells (2×10^5) that had been grown in DMEM culture medium supplemented with 10% FBS/100 units/ml penicillin/100 μg/ml streptomycin were seeded on glass coverslips coated with polyamino acids. The transfection procedures were performed according to the manufacturer's (GIBCO/BRL) recommendations by using 5 μg of Lipofectamine and either 1 μg of the pEGFP-N1-ACC2-N or pEGFP-N1-ACC1-N plasmid DNA. The culture medium was changed after 16 h, and the cells were transferred to growth medium and maintained for another 48 h to allow optimal expression of the fusion protein. The transfected cells that had adhered to the coverslips were stained with 5 μg/ml DAPI and were examined under a Zeiss Axiophot fluorescence microscope, which showed the cells to be fluorescent. All experimental conditions were the same for the rat neonatal cardiomyocytes, except that they were transfected for only 4 h.

Hydrophobic Profile of the Predicted Amino Acid Sequence of the N-Terminal Region of ACC2. Sequences were aligned by using the CLUSTALW program (27). The hydrophobicity plot was calculated by using Kyte–Doolittle (28) free-energy values that were averaged over a nine-residue window.

Results

When we compared the predicted amino acid sequence of human ACC2 with that of ACC1 we found that the N terminus of ACC2 was 114 aa longer than that of ACC1. Aside from these additional residues, the remaining amino acid sequences of ACC2 and ACC1 were very homologous, beginning at residues 217 and 77, respectively (6, 7). We took advantage of this variance at the N-terminal ends of the isozymes to produce polyclonal antibodies that would recognize ACC2 but not ACC1 (7). These antibodies reacted with the rat and mouse ACC2s (7), suggesting that the amino acid sequence at the N terminus of ACC2 is highly conserved among animal ACC2s, including the human enzyme. Examining the peptide segments from these additional amino acids at the N termini of ACC2 and ACC1 revealed that the first 150 aa of ACC2 have unique features. The hydropathic plot (28) of the 300 N-terminal amino acids of ACC2 showed that the peptide segment containing the first 20 aa is characteristically very hydrophobic; the next 20–100 aa form a long peptide segment that is characteristically hydrophilic (Fig. 1). The presence of this hydrophobic leader sequence suggested that ACC2 may be targeted to a membranous component of the cell. In contrast, the N-terminal amino acid segment (residues 1–50) of ACC1 was highly hydrophilic (Fig. 1), suggesting that ACC1 is not a membrane-bound enzyme as we demonstrate it to be below. It is noteworthy that the hydropathic profiles of ACC2 and ACC1 display a close similarity between the two carboxylases, beginning with about residue 150 of ACC2 and residue 10 of ACC1 (Fig. 1). This finding reaffirms our earlier conclusion that the two carboxylases are highly homologous (7).

The affinity-purified anti-ACC2 antibodies specific for the unique N-terminal peptide (7) were used to determine the intracellular localization of ACC2. Human cell lines HepG2 and T47D and neonatal rat cardiomyocytes were grown in culture medium, fixed on glass slides, and treated first with the primary

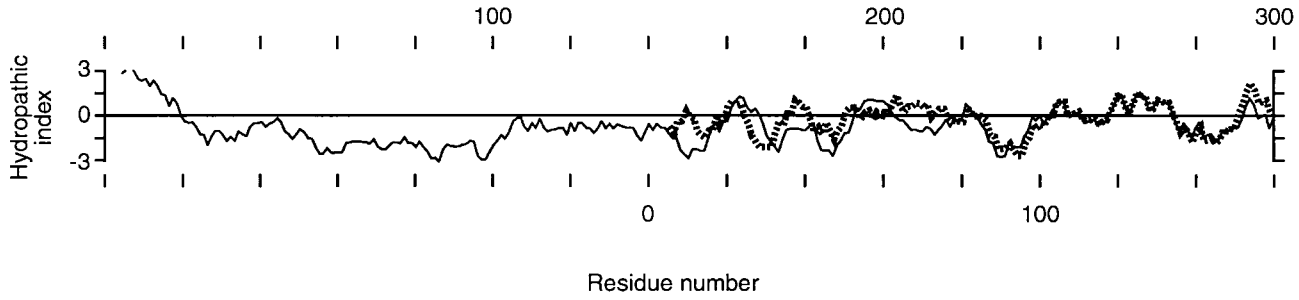

Fig. 1. Hydropathic profiles of the 300-residue N terminus of ACC2 (solid line) and the 160-residue N terminus of ACC1 (dotted line) according to Kyte and Doolittle (28) free-energy values. The sequence alignment was used as a basis for aligning the hydrophobicity plots of the N termini of ACC2 and ACC1.

antibodies or mAbs against a human mitochondria-specific protein (or both) and then with conjugated secondary antibodies as described in *Materials and Methods*. Microscopic images of the cells were collected and processed digitally. These images show that in human HepG2 cells the preimmune rabbit antibodies stained only the nucleus (Fig. 2*A*). On the other hand, the affinity-purified anti-ACC2 antibodies stained the nucleus and particulate cytoplasmic components of the cell (Fig. 2*D*). These labeled particulate components have the same distribution and appearance as those recognized by the mAbs against the 66-kDa human mitochondria-specific protein, suggesting that they are mitochondria (Fig. 2*E*). When the cells were treated with both the conjugated anti-ACC2 antibodies, which emit green fluorescence, and the conjugated monoclonal antimitochondrial protein antibodies, which emit red fluorescence, the two antibodies recognized the same particles as shown by the emission of yellow fluorescence in areas in which the images overlapped (Fig. 2*F*), suggesting their colocalization on the same cellular organelles, namely, the mitochondria. Similar results were obtained when we used human breast cancer T47D cells (Fig. 2 *G*–*J*), rat cardiomyocytes (Fig. 2 *K*–*N*), and mouse skeletal muscle tissue (Fig. 2*O*). It is interesting that the anti-ACC2 antibodies we used stained only the mitochondria of neonatal rat cardiomyocytes (Fig. 2 *L* and *N*) but not the nucleus, as occurred in human cells (Fig. 2 *A*, *D*, *F*, *H*, and *J*).

To demonstrate that the unique N-terminal peptide leader sequence of ACC2 is directing ACC2 toward the mitochondria, we cloned a cDNA fragment of ACC2 (nucleotides 1–1,250) into the pEGFP-N1 mammalian expression vector and generated the plasmid pEGFP-N1-ACC2-N as described in *Materials and Methods*. Expressing this construct in HepG2 cells yielded a fusion protein that had the expected molecular mass of 60 kDa based on the results of SDS/PAGE and a Western blot assay by using ACC2 antibodies (data not shown).

To determine whether the ACC2-GFP fusion protein is localized to the mitochondria, we expressed the pEGFP-N1-ACC2-N plasmid in human HepG2 cells and in rat neonatal cardiomyocytes and examined them under a fluorescence microscope. HepG2 cells that had been transfected with the control plasmid pEGFP-N1 exhibited a strong green fluorescent signal throughout the cells (Fig. 3*A*). Transfecting the cells with the pEGFP-N1-ACC2-N construct showed the green fluorescent product ACC2-GFP to be localized to specific sites in the cytosol (Fig. 3*C*). To show that these sites, where the ACC2 protein was located (Fig. 2), were mitochondrial, the cells were treated in succession with antibodies against ACC2 and stained with conjugated goat anti-rabbit IgG-TXRD antibodies (Fig. 3*D*); examining these cells by fluorescence microscopy disclosed that ACC2 and the ACC2-GFP fusion protein were located in the same organelles (Fig. 3 *C* and *D*). Converging the two images (Fig. 3 *C* and *D*) gave a yellow fluorescent pattern, confirming the colocation of the ACC2-GFP and ACC2 proteins (Fig. 3*E*). In contrast, when the pEGFP-N1-ACC1-N plasmid expressing ACC1-GFP was used to transfect the HepG2 cells, the expressed fusion protein was not targeted to the mitochondria; instead, the fusion protein was expressed and localized in the cytosol (Fig. 3*G*) in a pattern similar to that of the control plasmid pEGF-N1 (Fig. 3*A*).

The finding that ACC2 is associated with the mitochondria and the prevailing concept that malonyl-CoA regulates the activity of CPT1 stimulated us to investigate the cellular colocation of the two enzymes. Polyclonal antibodies prepared against human CPT1 that was isolated from the mitochondrial membranes of human heart muscle cells and recognized CPT1 as a single band in a Western blot (25) were used in immunofluorescence microscopy. As shown in Fig. 4, the anti-CPT1 antibodies were bound to the mitochondria of the human HepG2 cells as detected with the green fluorescent goat anti-rabbit IgG-FITC conjugate (Fig. 4*A*). As expected, the mAbs against the 66-kDa human mitochondria-specific protein detected with the goat anti-mouse IgG-TXRD conjugate identified the mitochondria (Fig. 4*B*). However, CPT1 antibodies recognized additional sites, suggesting that CPT1 may not be localized exclusively to the mitochondrial membrane (29). When the two images (Fig. 4 *A* and *B*) were converged, the mitochondrial CPT1-specific antibodies could be detected as shown by the bright yellow fluorescence (Fig. 4*C*). Similarly, most of the red and green fluorescence was colocalized to the same mitochondrial particles when the cells were transfected with pEGFP-N1-ACC2-N (Fig. 4*E*) and probed with CPT1 antibodies that were stained with the goat anti-rabbit IgG-TXRD conjugate (Fig. 4 *F* and *G*).

Discussion

Of the two ACC isoforms found in animals, ACC1 is the dominant isoform in lipogenic tissues such as liver, adipose, mammary gland, and lung, whereas ACC2 is the major isoform expressed in heart, muscle, and, to a lesser extent, liver (4, 5, 7, 9). In animal tissues, malonyl-CoA, the product of ACC1 and ACC2, plays an interesting metabolic role by integrating the two opposite pathways of fatty acid metabolism, synthesis and oxidation. In the liver and other lipogenic tissues, malonyl-CoA is synthesized by ACC1 in the cytoplasm and is the source of the C_2 units that are the building blocks of fatty acid synthesis (1, 30, 31). Malonyl-CoA is synthesized by ACC2 in the heart, muscle, and liver and is probably the regulator of the carnitine palmitoyl-CoA shuttle system. This system, first discovered by Fritz in 1955 (32), is involved in the transfer of the palmitoyl group from palmitoyl-CoA within the cytosol to the mitochondrial matrix, where it is oxidized by the β-oxidation system. This shuttle system is catalyzed by CPT1 and CPT2, which are associated with the mitochondrial membrane (24). CPT1, which is located

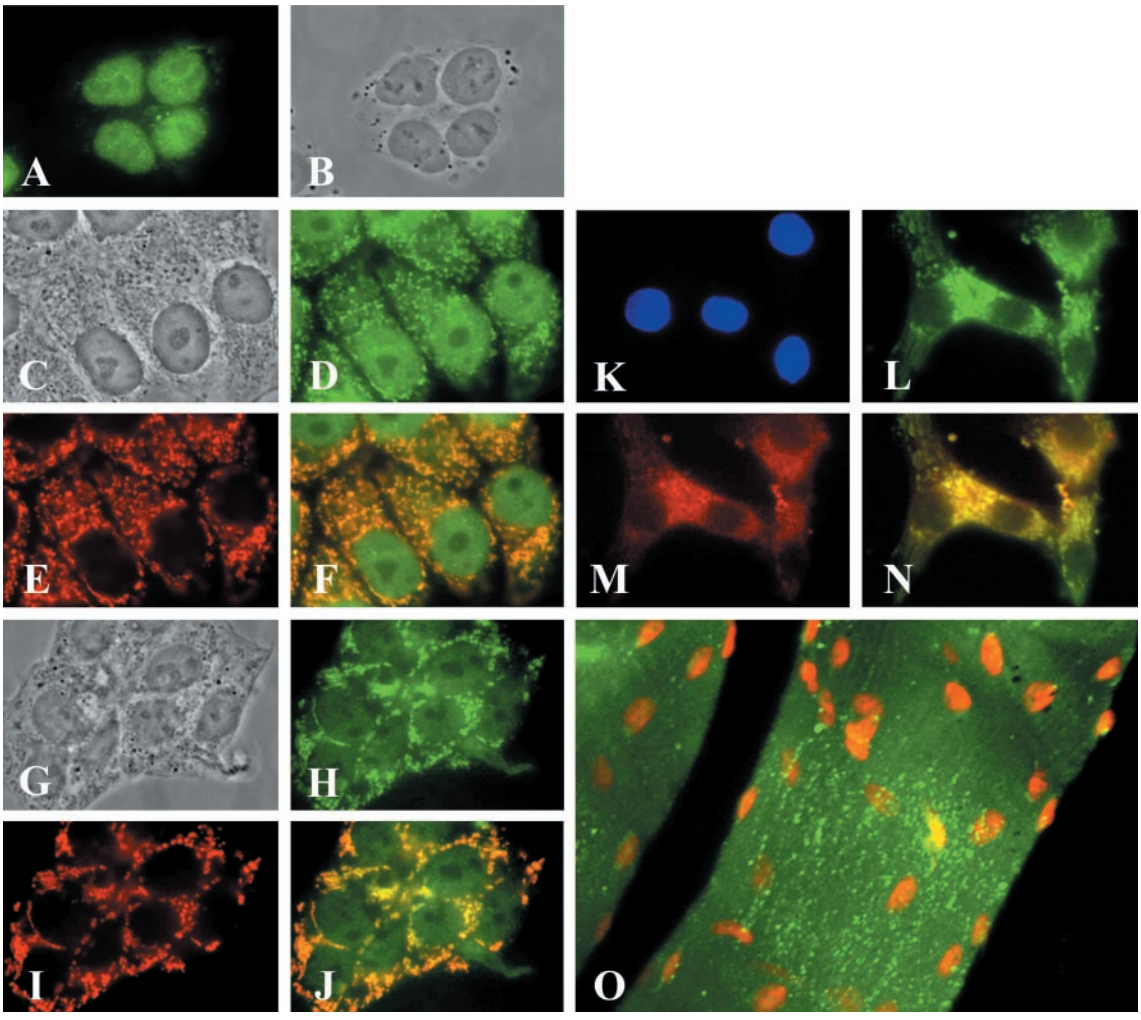

Fig. 2. Determination of the mitochondrial localization of ACC2 by fluorescence microscopic analysis. HepG2 cells (*A*–*F*), T47D cells (*G*–*J*), and neonatal rat cardiomyocytes (*K*–*N*) were plated separately at a density of 2×10^5 on glass coverslips coated with polyamino acids. After 48 h of incubation in medium containing 10% bovine serum, the cells were fixed in 3.7% formaldehyde and then immunostained with preimmune serum (*A*) or ACC2 antibodies and mAbs raised against mitochondria-specific protein as a marker (*D*, *E*, *H*, *L*, and *M*). The cells were visualized by reacting them with the goat anti-mouse IgG-TXRD conjugate for the mitochondrial proteins (red) or with the goat anti-rabbit IgG-FITC conjugate (green) for ACC2. (*B*, *C*, and *G*) The images were visualized by phase-contrast microscopy and clearly show the nuclei and cytoplasm of the cells. (*F*, *G*, and *N*) Composite images, respectively, of *D* and *E*, *H* and *I*, and *L* and *M*. The overlapping regions in *F*, *G*, and *N* are yellow. (*O*) Mouse skeletal muscle tissue that was immunostained with ACC2 antibodies and was visualized by reacting it with the goat anti-rabbit IgG-FITC conjugate (green). The nuclei of the skeletal muscle cells were stained with 0.5 μg of propidium iodide. (*K*) Neonatal rat cardiomyocytes were counterstained with DAPI.

on the outer surface of the mitochondrial membrane (29), transfers the cytoplasmic palmitoyl group from CoA to carnitine, yielding palmitoylcarnitine and free CoA. The palmitoylcarnitine is transported across the inner mitochondrial membrane and then is transferred to the matrix CoA to form carnitine and palmitoyl-CoA in a reaction that is catalyzed by CPT2, which is located on the matrix side of the mitochondrial membrane.

By catalyzing the transfer of palmitate from the cytosol to the mitochondrial matrix, the CPT system plays a pivotal role in fatty acid oxidation and energy production (24). The CPT1 reaction is the committed step in this shuttling process and, therefore, is subject to tight regulation. The key metabolite involved in CPT1 regulation is malonyl-CoA, a potent inhibitor of CPT1. Malonyl-CoA is also the donor of C_2 units for fatty acid synthesis (31). Thus, this interrelationship has provided a reasonable explanation for the balance between fatty acid synthesis and oxidation and has related them to carbohydrate and energy metabolism. For instance, a carbohydrate-rich diet raises the level of insulin, increases the rate of glycolysis, and stimulates greater production of malonyl-CoA through the activation of ACC1 and ACC2 by dephosphorylation and a rise in the level of citrate. Moreover, prolonged carbohydrate feeding leads to increased expression of the carboxylase and, hence, to increased production of malonyl-CoA, increased hepatic lipogenesis, and a decline in fatty acid mobilization and oxidation. Conversely, starvation and diabetes (a low insulin level and a high glucagon/insulin ratio) diminish glycolysis, stimulate fatty acid mobilization, and reduce ACC activity by phosphorylation. After prolonged starvation, ACC expression is repressed, the level of malonyl-CoA is greatly lowered, CPT1 activity is greatly increased, and fatty acid oxidation and ketone body formation are stimulated. Clearly, by being a common metabolite, malonyl-CoA interrelates fatty acid synthesis and oxidation.

The finding that there are two ACC isoforms raises questions about the roles each of them plays in fatty acid metabolism. Because ACC2 is highly expressed in heart and skeletal muscle and because very little fatty acid synthesis takes place in these tissues, ACC2 is the most likely source of the malonyl-CoA that

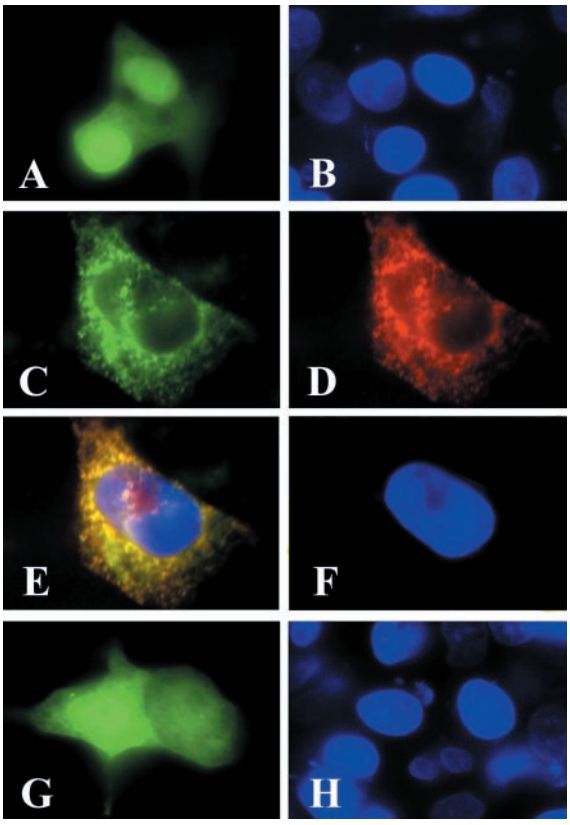

Fig. 3. The ACC2 N terminus directs the GFP to the mitochondria. Neonatal rat cardiomyocytes were plated at a density of 2×10^5 on glass coverslips as described in the legend to Fig. 2. The cells were transfected with 1 μg/ml pEGFP-N1 (*A* and *B*), pEGFP-N1-ACC2-N (*C* and *D*), or pEGFP-N1-ACC1-N (*G* and *H*) by using the transfection reagent Lipofectamine according to the manufacturer's protocol. After 48 h of transfection, the cells were examined by fluorescence microscopy to verify expression of the GFP fusion protein (green). Cells that were transfected with pEGFP-N1-ACC2-N were immunostained with ACC2 antibodies and visualized by reacting them with the goat anti-rabbit IgG-TXRD conjugate (*D*). (*E*) A composite image of *C* and *D*; the overlapping regions in *E* are yellow. The cells were counterstained with DAPI (blue).

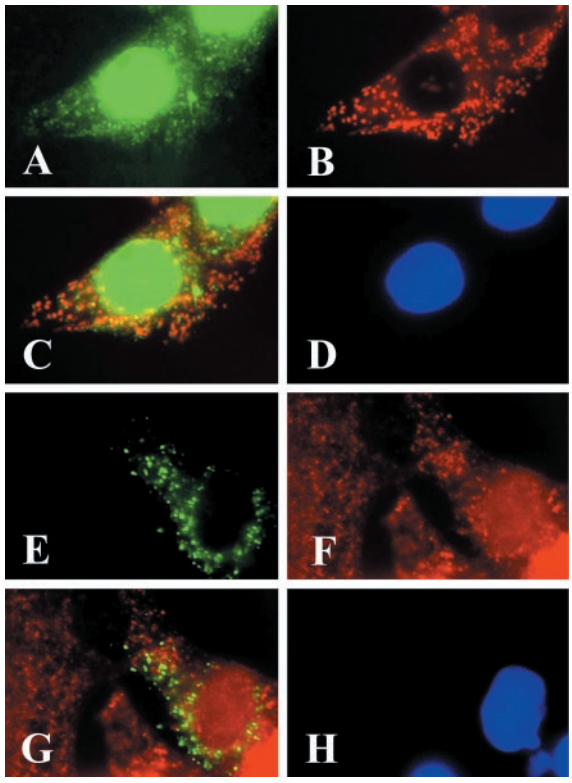

Fig. 4. CPT1 and the GFP1-N1-ACC2-N fusion protein are colocalized on the mitochondria. HepG2 cells were plated at a density of 2×10^5 on glass coverslips for immunostaining and transfection as described in the legends to Figs. 2 and 3. The cells were immunostained with CPT1 antibodies that were detected by reacting the cells with the goat anti-rabbit IgG-FITC conjugate (*A*) and with mAbs raised against the mitochondrial protein and were visualized by reacting them with the goat anti-mouse IgG-TXRD conjugate (*B*). (*C*) A composite image of *A* and *B*; the overlapping regions in *C* are yellow. In the transfection experiments, the cells were transfected with pEGFP-N1-ACC2-N, as described in *Materials and Methods*, and were immunostained with CPT1 antibodies. The expressed GFP-N1-ACC2-N is green (*E*). Immunostaining of CPT1 was detected by reacting the cells with the goat anti-rabbit IgG-TXRD conjugate (*F*). (*G*) A composite image of *E* and *F*; the overlapping regions in *G* are yellow. The cell nuclei were counterstained with DAPI (blue in *D* and *H*).

is responsible for the regulation of fatty acid oxidation. Evidence presented in this communication strongly supports this proposition. What specifically suggested ACC2 to be a membrane-targeted enzyme were the findings that the predicted amino acid sequence of the NH_2 terminus of ACC2 contains 114 aa more than that of ACC1 (7, 9) and that the first 20 aa of this NH_2-terminal peptide of ACC2 are remarkably hydrophobic and are followed by a hydrophilic stretch of about 100-aa peptide residues (Fig. 1). These are two characteristic properties needed to target a protein to cellular membranes (33). It is noteworthy that when the predicted amino acid sequences of ACC1 and ACC2 were examined for their hydropathic profiles (28), the predicted hydrophobic and hydrophilic profiles of ACC2 and ACC1 were remarkably similar, except for the NH_2-terminal sequence of the first 140 aa residues of ACC2 (Fig. 1).

The hydrophobic N-terminal leader sequence targets ACC2 to the mitochondrial membrane and enhances its attachment to and anchoring in the membrane. Because this hydrophobic leader sequence is immediately followed by a 100-aa hydrophilic peptide (Fig. 1), it is tempting to suggest that the leader sequence functions solely to anchor ACC2 in the membrane, with the bulk of the polypeptide facing the cytosol, where it receives its substrate acetyl-CoA and is subjected to phosphorylation/dephosphorylation and allosteric regulation. With this anchoring leader sequence, it is reasonable to assume that ACC2 is associated with the cytoplasmic side of the mitochondrial membrane or, rather, the contact sites of the outer and inner mitochondrial membranes as suggested by Hoppel *et al.* (29). This association can be readily reversed, because the bulk of the molecule is exposed to the outside of the membrane. This may be the reason why previous attempts to establish a subcellular localization of ACC2 have been difficult; most of the isolation procedures used thus far have involved harsh treatments (29). Interestingly, the proposed model for the membrane topology of CPT1 predicts exposure of 90% of the enzyme, including N- and C-terminal domains crucial for activity and malonyl-CoA sensitivity, on the cytosolic side of the outer mitochondrial membrane (34, 35).

In the present study, by using affinity-purified antibodies and immunocytochemical protocols we determined the *in vivo* cellular distribution of ACC2 in different animal cells, including neonatal rat cardiomyocytes, mouse skeletal muscle tissues, and human cancer cell lines HepG2 and T47D. The protocol we employed enabled us to detect specifically very small amounts of ACC2 *in situ*. Moreover, to prevent potential contamination of the mitochondria with nonmitochondrial proteins, the cells were fixed before they were treated with detergent that disrupts the

cell membrane. Our results show that affinity-purified anti-ACC2 antibodies stain the cellular particles of human HepG2 cells, human T47D cells, neonatal rat cardiomyocytes, and mouse skeletal muscle tissues (Fig. 2). We identified these particles as mitochondria because antibodies against a mitochondria-specific protein stained them and because these antibodies and the anti-ACC antibodies both cospanned the same particle (Fig. 2). We demonstrated that the leading NH_2-terminal peptide is sufficient to direct ACC2 to its mitochondrial site by using the human ACC2-GFP expression plasmid construct pEGFP-N1-ACC2-N, which contained GFP cDNA that had been fused to the 3′ end of a cDNA segment that contained the first 1,250 nt of ACC2 cDNA. Expressing this plasmid in HepG2 cells and in neonatal rat cardiomyocytes yielded a 60-kDa fusion protein that contained GFP and the NH_2-terminal segment of ACC2. Examining these cells by fluorescence microscopy showed that the expressed green protein was associated with cytoplasmic particles that were identified as the mitochondria at which ACC2 is located (Figs. 2 and 3).

As expected, CPT1 is associated with the mitochondria as shown by its colocalization with the mitochondria-specific protein (Fig. 4 *A*–*C*). To demonstrate that the ACC2 and CPT1 proteins colocalize on the mitochondria, we carried out similar immunocytochemical studies by using the GFP-N1-ACC2 expression system and anti-CPT1 antibodies (Fig. 4 *E*–*G*). Because both the ACC2 and CPT1 antibodies are generated in rabbits, we could not use anti-rabbit IgG for colocalization of the two enzymes. Instead, we took advantage of the GFP-N1-ACC2 fusion protein. Once again the CPT1 antibodies and GFP-N1-ACC2 stained the same particles, suggesting their colocalization on the mitochondria (Fig. 4 *E*–*G*). The costaining of the mitochondrial particles in these experiments was shown to be not as prevalent as that found in the experiments depicted in Figs. 2 and 3 because CPT1 may not be localized exclusively in the outer membrane of liver mitochondria, a conclusion similar to that of Hoppel *et al.* (29), who reported that CPT1 may be associated with contact sites of the outer and inner membranes of rat liver mitochondria. The close proximity between ACC2 and CPT1 is physiologically important for the regulation of CPT1 activity by the ACC2 product, malonyl-CoA. This close proximity is needed especially to regulate CPT1 activity and, hence, energy production in heart and muscle. The concentration of malonyl-CoA and the activity of ACC2 in skeletal muscle, for instance, are controlled rapidly during contraction of the muscle fibers by diminishing ACC2 activity by increasing its phosphorylation through the action of kinases (10–18, 36). A lower concentration of malonyl-CoA results in increasing CPT1 activity and, hence, in increased fatty acid oxidation and energy production, a condition needed in exercising animals (37).

In summary, the evidence presented herein indicates that ACC2, together with CPT1, is associated with the mitochondria, most likely on the outer membrane. Through this association, ACC2 provides the malonyl-CoA that allosterically regulates CPT1 activity and, hence, the process of fatty acid oxidation and energy production.

We are grateful to Dr. David A. Wheeler, director of the Molecular Biology Computational Resource at Baylor College of Medicine, for providing the hydropathic profile of ACC2 and to Pamela Paradis Tice, Editor in the Life Sciences, for editing the manuscript. This work was supported by Grants GM-19091 (S.J.W.), CA-41424 (W.R.B.), and HL-52571 (G.W.) from the National Institutes of Health and a grant from the Clayton Foundation for Research (S.J.W.).

1. Wakil, S. J. (1958) *Am. J. Chem. Soc.* **80,** 6465.
2. Nugteren, D. H. (1965) *Biochim. Biophys. Acta* **106,** 280–290.
3. Hopwood, D. A. & Sherman, D. H. (1990) *Annu. Rev. Genet.* **24,** 37–66.
4. Thampy, K. G. (1989) *J. Biol. Chem.* **264,** 17631–17634.
5. Bianchi, A., Evans, J. L., Iverson, A. J., Nordlund, A.-C., Watts, T. D. & Witters, L. A. (1990) *J. Biol. Chem.* **265,** 1502–1509.
6. Abu-Elheiga, L., Jayakumar, A., Baldini, A., Chirala, S. S. & Wakil, S. J. (1995) *Proc. Natl. Acad. Sci. USA* **92,** 4011–4015.
7. Abu-Elheiga, L., Almarza-Ortega, D. B., Baldini, A. & Wakil, S. J. (1997) *J. Biol. Chem.* **272,** 10669–10677.
8. Lopaschuk, G. D., Witters, L. A., Itai, T., Barr, R. & Barr, A. (1994) *J. Biol. Chem.* **269,** 25871–25878.
9. Ha, J., Lee, J.-K., Kim, K.-S., Witters, L. A. & Kim, K.-H. (1996) *Proc. Natl. Acad. Sci. USA* **93,** 11466–11470.
10. Thampy, K. G. & Wakil, S. J. (1988) *J. Biol. Chem.* **263,** 6447–6453.
11. Thampy, K. G. & Wakil, S. J. (1988) *J. Biol. Chem.* **263,** 6454–6458.
12. Lopez-Casillas, F., Bai, D.-H., Luo, X., Kong, I.-S., Hermodson, M. A. & Kim, K.-H. (1988) *Proc. Natl. Acad. Sci. USA* **85,** 5784–5788.
13. Takai, T., Yokoyama, C., Wada, K. & Tanabe, T. (1988) *J. Biol. Chem.* **263,** 2651–2657.
14. Hardie, D. G. (1989) *Prog. Lipid Res.* **28,** 117–146.
15. Kim, K.-H., Lopez-Casillas, L. A., Bai, D. H., Luo, X. & Pape, M. E. (1989) *FASEB J.* **3,** 2250–2256.
16. Mabrouk, G. M., Helmy, I. M., Thampy, K. G. & Wakil, S. J. (1990) *J. Biol. Chem.* **265,** 6330–6338.
17. Quayl, K. A., Denton, R. M. & Brownsey, R. W. (1993) *Biochem. J.* **292,** 75–84.
18. Mohamed, A. H., Huang, W.-Y., Huang, W., Venkatachalam, K. V. & Wakil, S. J. (1994) *J. Biol. Chem.* **269,** 6859–6865.
19. Mosoro, E. J. & Porter, E. (1965) *Proc. Soc. Exp. Biol. Med.* **118,** 1090–1095.
20. Wit-Peeters, E. M., Scholte, H. R. & Elenbass, H. L. (1970) *Biochim. Biophys. Acta* **210,** 360–370.
21. Winz, R., Hess, D., Aebersold, R. & Brownsey, W. (1994) *J. Biol. Chem.* **269,** 589–594.
22. Witters, L. A., Widmer, J., King, A. K., Fassihi, K. & Kuhajda, F. (1994) *Intl. J. Biochem.* **26,** 589–594.
23. McGarry, J. D., Mannaerts, G. P. & Foster, D. W. (1977) *J. Clin. Invest.* **60,** 265–270.
24. McGarry, J. D. & Brown, N. F. (1997) *Eur. J. Biochem.* **244,** 1–14.
25. Zhu, H., Shi, J., de Vries, Y., Arvidson, D. N. & Woldegiorgis, G. (1997) *Arch. Biochem. Biophys.* **347,** 53–61.
26. Van Hooser, A. & Brinkley, W. R. (1999) *Methods Cell Biol.* **61,** 57–80.
27. Thompson, J. D., Higgins, D. G. & Gibson, T. J. (1994) *Nucleic Acids Res.* **22,** 4673–4680.
28. Kyte, J. & Doolittle, R. F. (1982) *J. Mol. Biol.* **157,** 105–132.
29. Hoppel, C. L., Kerner, J., Turkaly, P., Turkaly, J. & Tandler, B. (1998) *J. Biol. Chem.* **273,** 23495–23503.
30. Wakil, S. J., Stoops, J. K. & Joshi, V. C. (1983) *Annu. Rev. Biochem.* **52,** 537–579.
31. Wakil, S. J. (1989) *Biochemistry* **28,** 4523–4530.
32. Fritz, I. (1955) *Acta Physiol. Scand.* **34,** 367–385.
33. Heijne, G. V. (1985) *Curr. Top. Membr. Transp.* **24,** 151–179.
34. Shi, J., Zhu, H., Arvidson, D. & Woldegiorgis, G. (1999) *J. Biol. Chem.* **274,** 9421–9426.
35. Faser, F., Corstorphine, C. G. & Zammit, V. A. (1997) *Biochem. J.* **323,** 711–718.
36. Dyck, J. R. B., Kudo, N., Bare, A. J., Davies, S. A., Hardie, D. G. & Lopaschuk, G. D. (1999) *Eur. J. Biochem.* **262,** 184–190.
37. Greelen, M. J., Bijleveld, C., Velasco, G., Wanders, R. J. & Guzamán, M. (1997) *Biochem. Biophys. Res. Commun.* **233,** 253–257.